Since January 2020 Elsevier has created a COVID-19 resource centre with free information in English and Mandarin on the novel coronavirus COVID-19. The COVID-19 resource centre is hosted on Elsevier Connect, the company's public news and information website.

Journal of Biomechanics 112 (2020) 110037

Contents lists available at ScienceDirect

Journal of Biomechanics

journal homepage: www.elsevier.com/locate/jbiomech
www.JBiomech.com

Prediction of upper airway dryness and optimal continuous positive airway pressure conditions

Sandra Grau-Bartual, Ahmed M. Al-Jumaily *

Institute of Biomedical Technologies, Auckland University of Technology, Auckland, New Zealand

ARTICLE INFO

Article history:
Accepted 1 September 2020

Keywords:
Human epithelial cells
Continuous positive airway pressure (CPAP)
Humidification
Upper airway dryness
Heat and mass transfer

ABSTRACT

Continuous positive airway pressure is the most effective long-term treatment for obstructive sleep apnoea, which is a sleeping disorder characterized by pauses in breathing during sleep. It introduces pressurized atmospheric air into the respiratory system in order to maintain open airways without blockage. Some continuous positive airway pressure devices incorporate a convective heat transfer humidifier to overcome dryness. However, many side effects, including the unacceptable excess of water droplets in the air supply line, have been reported and improvements are essential for better patient's comfort and acceptance of the therapy. The excess of water droplets is attributed to the qualitative rather than the quantitative approach of determining the rise in temperature and humidity of the inspired air. Therefore, a human upper airway mathematical model is developed to predict the heat and water transfer variation between normal breathing and continuous positive airway pressure conditions and determine the optimal input temperature and relative humidity in the continuous positive airway pressure humidifier.

1. Introduction

Lung supportive devices, such as nebulizers, positive airway pressure devices or respirators are used to restore the respiration cycle, alleviate symptoms and associated morbidities of some patients. Continuous positive airway pressure (CPAP) is the most effective long-term treatment for obstructive sleep apnoea (Al-Jumaily et al., 2003), which is a sleeping disorder characterized by pauses in breathing during sleep. It occurs when the muscles relax causing soft tissue in the back of the throat to collapse and block the upper airway (UA) (West, 2013). A CPAP device is composed of an air pump connected to a nasal or facial mask. The principal function is to introduce atmospheric air at a specific pressure into the respiratory system in order to maintain the airway patency and avoid blockage. Several nasal symptoms such as dryness, sneezing, rhinorrhoea, post-nasal drip, nasal congestion or epistaxis are often reported by CPAP patients. Those patients describe the symptoms as similar to an upper respiratory tract infection, *i.e.* like having a cold (Malik and Kenyon, 2004).

Airways dryness, as a side effect of CPAP use, is normally attributed to inefficient UA air conditioning. This is a transport process which controls the temperature and the humidity of the air during respiration. During inspiration, air is in contact with the warm and moist nasal mucosa and is rapidly warmed and humidified. This heat and mass transfer process is produced due to the driving force created by the difference in temperature and water concentration between the inspired air, which is at room temperature and humidity (Wolf et al., 2004) and the airway surface liquid layer, which is composed of 95% water and 5% of carbohydrate, protein, lipid and inorganic material at body temperature (Yeager, 1971; Reinikainen and Jaakkola, 2003). During expiration air loses heat and water to the outside. However, under CPAP there is an increase in turbulent effect during inspiration and the air introduced in the respiratory system has higher pressure than during normal breathing. This high pressure temporarily deforms the respiratory tissue and may close the secreting cells, which may block the mucus secretion and hinder natural lubrication and normal air-conditioning of the airway.

To improve the comfort and the acceptance of patients, convective heat transfer humidifiers are incorporated into CPAP devices in order to provide an additional humidification to the room air introduced into the respiratory system (Reinikainen and Jaakkola, 2003; F&P, 2012). Therefore, a failure in the conditions of the air under CPAP therapy and the dryness side effect are currently corrected

* Corresponding author at: Biomechanical Engineering, Director, Institute of Biomedical Technologies, Auckland University of Technology, Private Bag 92006, Wellesley Campus, WT612 Auckland, New Zealand.
E-mail address: ahmed.al-jumaily@aut.ac.nz (A.M. Al-Jumaily).

https://doi.org/10.1016/j.jbiomech.2020.110037
0021-9290/

Nomenclature

A	Upper airway cross-sectional area, $\pi(D/2)^2$ [cm^2]
B	Bulk modulus of respiratory epithelium [Pa]
C	Concentration [mol/cm^3]
C_p	Heat capacity at constant pressure [cal/g K]
CCA	Epithelial circular crown area [nm^2]
D	Upper airway diameter [cm]
Dif	Diffusivity of water vapour in air [cm^2/s]
h_C	Heat transfer coefficient, $Nu\ k_A/D$ [cal/cm^2 s K]
h_{fg}	Latent heat of vaporization [cal/g]
k	Thermal conductivity [cal/cm s K]
k_C	Mass transfer coefficient, $Sh\ Dif/D$ [cm/s]
L	Upper airway length [cm]
M	Molecular weight [g/mol]
N	Mass transfer rate [$mol/cm^3 s$]
Nu	Dimensionless Nusselt number, $3.504(Re\ D/D_{10})^{0.277}$ (Wu et al., 2014)
P	Pressure [cmH_2O]
q	Heat rate [cal/s]
Q	Airflow rate [cm^3/s]
R	Ideal gas constant [m^3Pa/mol K]
Re	Dimensionless Reynolds number
rH	Relative humidity [%]
ρ	Moist air density [g/cm^3]
Sh	Dimensionless Sherwood number, $3.652(Re\ D/D_9)^{0.268}$ (Guimarães et al., 2009)
T	Temperature [K]
V	Epithelial volume [nm^3]
v	Velocity, $Q_{\Delta P}/A$ [cm/s]
y_{ASL}	ASL thickness [nm]
y_{Ep}	Epithelial thickness [nm]

Subscripts

A	Moist airflow
B	Blood
CD	Conduction heat
CV	Convection heat
fg	Vaporization heat
ΔP	Positive airway pressure increase [0, 5, 10, 15 or 20]
k	Segment number [1, 2, 3, 4, 5, 6, 7, 8, 9 or 10]
M	Mucus
sat	Saturation conditions
W	Water

by increasing the inlet temperature and humidity of the inspired air to help the airflow to reach 37 °C and 44 mgH_2O/L at the main bronchi. Current practice incorporates a user interface to control the temperature and humidity simultaneously in a scale which varies between manufacturers. As an example, F&P Icon CPAP uses a scale of 0–7, where 0 corresponds to the humidifier off position and 7 to the maximum humidity and temperature setting. The user normally sets the scale by "trial and error" until the comfort level is reached. However, this qualitative adjustment may lead to uncomfortable breathing or possible risky excess water droplets in the breathing air supply line.

One-dimensional (1D), two-dimensional (2D) and three-dimensional (3D) computational models for temperature and water vapour concentration have previously been developed to study the air conditioning characteristics of the human respiratory tract. 1D and 2D models are more widely used methods due to their simplicity and efficiency, where air temperature and water vapour concentration are obtained by solving scalar transport equations and energy balance equations based on control volume analysis (Hanna and Scherer, 1986; Daviskas et al., 1990). 3D models are computationally more demanding because they provide detailed air distributions of velocities, temperature and water vapour concentration, but the computational time and model size is greater compared to 1D models (Feng et al., 2016; Xi et al., 2016; Wu et al., 2014).

The purpose of this research is to develop a simple, efficient, fast computing and realistic 1D upper airway mathematical model which can predict the heat and water transfer variation between normal breathing and under CPAP conditions. It is expected that the model is used to predict the optimal input temperature and relative humidity in the CPAP humidifier to overcome the dryness side effect and improve the patient's comfort and acceptance of CPAP.

2. Model description and assumptions

To facilitate model development, assumptions and simplifications are made to reduce computational complexity whilst maintaining the governing process characteristics. These include: (i) The geometry of the human upper airways has been approximated to an idealized symmetric cylinder-based airway model using data previously reported by the literature (Hanna and Scherer, 1986; Daviskas, Gonda and Anderson, 1990; Yu, Lau and Nikezic, 2006). Each cylinder is assumed uniform and represents one of the areas of interest in the upper airways, including: nasal vestibule, nasal cavity, nasal turbinate, proximal nasopharynx, distal nasopharynx, oropharynx, hypopharynx, larynx, proximal trachea and distal trachea (airway model outlined in Fig. 1). (ii) Axial conduction and convection heat along the airway are assumed to be negligible, while the radial conduction and convection heat are the main sources of energy (Hanna and Scherer, 1986; Daviskas, Gonda and Anderson, 1990; Yu, Lau and Nikezic, 2006). (iii) Air and water vapour mixture is considered as an ideal gas, one-dimensional and homogeneous at the end of each cylinder-based segment. (iv) Airway surface liquid (ASL) and epithelial cell layers are considered as a unique homogeneous layer due to the similarities in composition, since both are composed by 95% of water (Even-Tzur et al., 2008; Kreda et al., 2007), and the water content on the ASL outer surface in contact with the airflow is considered in thermodynamic liquid–vapour phase equilibrium. (v) The relative thicknesses of the ASL, epithelial layer, and basement membrane are assumed constant for all cylinders, but different for each positive airway pressure simulated. (vi) The airflow process is considered time-independent, steady, and fully developed, simulating only inspiratory phase, hence the gas is moving from the nares to the trachea. This simplification is made to achieve model validation with the previous *in vitro* results (Grau-Bartual et al., 2020). The model is formulated to simulate a nasal respiration only and is solved for steady-state conditions.

3. Governing equations

Conservation of mass, momentum and energy are used to determine water vapour and heat exchange between the ASL and the airflow under 0, 5, 10, 15 and 20 cmH_2O CPAP pressures. Zero cmH_2O CPAP pressure is considered to simulate the normal breathing conditions. The heat and water transfer fluxes in x and y directions along with state variables and parameters considered for physical modelling of the human breathing conditions are outlined in Fig. 2.

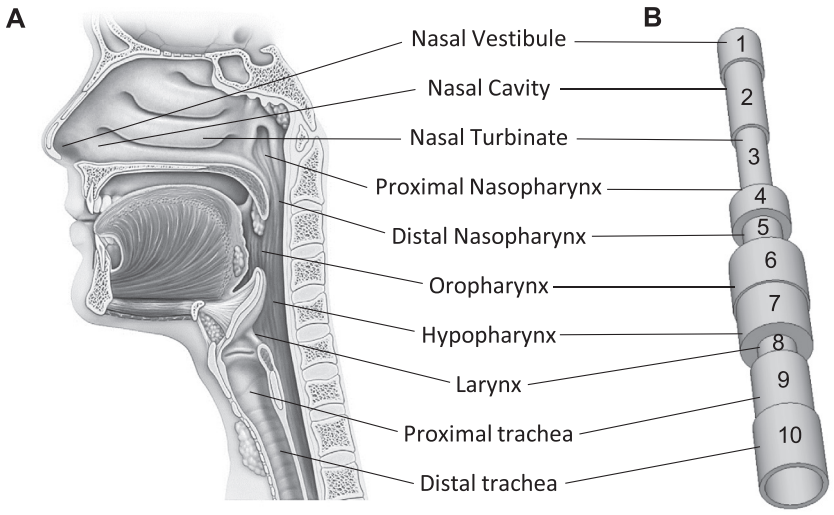

Fig. 1. Description of the human upper airway regions of interest used to develop the geometrical modelling. (A) Human upper airways anatomy (The anatomy and body, 2018). (B) The idealized symmetric cylinder-based airway model.

Three heat fluxes per unit area and time are considered in the y-axis: conductive sensible heat from the blood capillary terminals through the epithelium (q_{CD}), convective sensible heat from the ASL outer surface to the airflow (q_{CV}) and latent heat involved in water liquid–gas phase change (q_{fg}). Applying conservation of energy across the epithelium and ASL the heat balance can be written as follows:

$$\frac{k_M}{y_{Ep}}(T_B(x) - T_M(x)) = h_C(x)(T_M(x) - T_A(x)) + h_{fg}M_W N(x) \quad (1)$$

where y_{Ep} is the epithelium thickness, k_M is the thermal conductivity, h_C is the heat transfer coefficient, h_{fg} is the water latent heat of vaporization, M_W is the water molecular weight and T_B, T_M, and T_A are the basement capillary membrane temperature, mucus temperature at the ASL outer surface and airflow temperature, respectively.

The mass transfer rate or water molar flux (N) is by definition the convective mass transfer flux generated as a consequence of the water concentration gradient from the ASL outer surface (C_M) to the airflow (C_A) at specific mass transfer coefficient (k_C) *i.e.* the amount of water transferred from the ASL or mucus layer to the breathing airflow per unit volume and time. It can be written as follows:

$$N(x) = k_C(x)(C_M(x) - C_A(x)) \quad (2)$$

The water concentration at the ASL outer surface, *i.e.* mucus-air interface, (C_M) is determined by the thermodynamic water liquid–vapour phase equilibrium at saturation conditions. The saturation pressure of the liquid–vapour equilibrium is determined by the

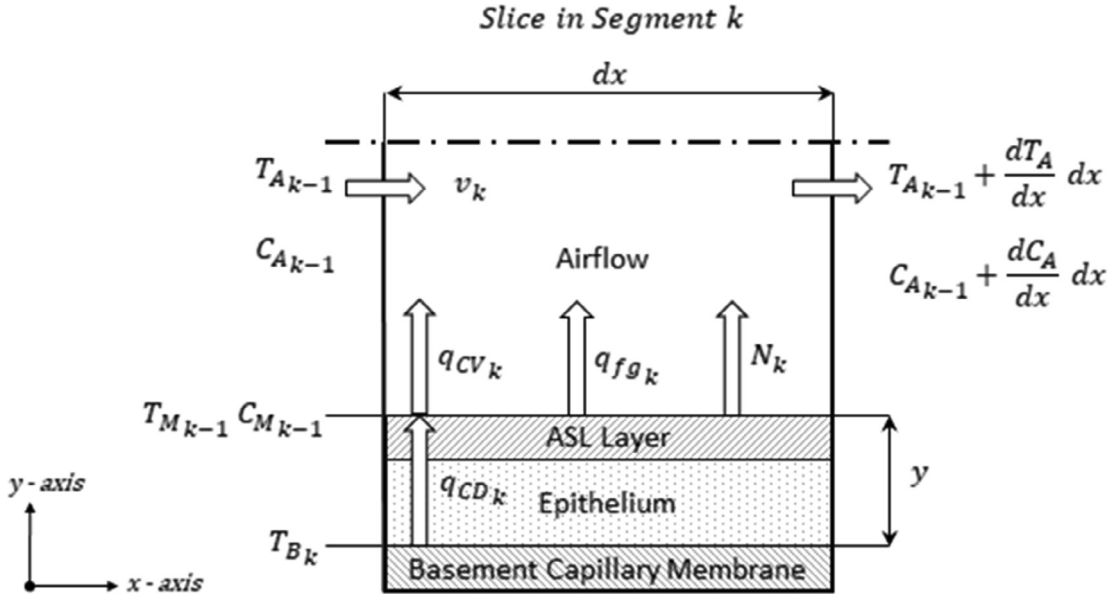

Fig. 2. Schematic representation of conduction, convection and vaporization heat (q_{CD}, q_{CV}, q_{fg}, respectively) and water transfer (N) fluxes in a *dx* slice of the segment k, and state variables such as airflow, ASL outer surface and blood temperatures (T_A, T_M, T_B, respectively) and water concentration on the airflow and ASL layer (C_A, C_M, respectively) at the airway distance*x*.

empirical Tetens equation (Buck, 1981), which relates the saturation water vapour pressure with the temperature improving the Clapeyron equation. Hence, the water concentration at mucus-air interface is written as:

$$C_M(x) = \frac{0.611 \cdot 10^{-3}}{RT_M(x)} \cdot \exp\left(\frac{17.27(T_M(x) - 273.15)}{(T_M(x) - 273.15) + 237.3}\right) \quad (3)$$

Finally, mass and energy balances are performed on the air phase of each *dx* slice on the x-axis giving respectively:

$$v(x)\frac{dC_A}{dx} = \frac{4}{D(x)} k_C(x)(C_M(x) - C_A(x)) \quad (4)$$

$$v(x)\frac{dT_A}{dx} = \frac{4}{D(x)\rho C_{pA}}\left(h_C(x)(T_M(x) - T_A(x)) + C_{pW} M_W N(x)(T_M(x) - T_A(x))\right) \quad (5)$$

where v is the local mean airflow velocity across the airways, D is the cross-sectional diameter, ρ is the air density and C_{pA} and C_{pW} are the air and water heat capacitances at constant pressure respectively.

Therefore, the theoretical model is managed by five main Eqs. (1)–(5) which are used to determine the five state variables (T_A, T_M, C_A, C_M, N) along the upper airways.

4. Boundary conditions

Two boundary conditions are set to characterize the upper airway inlet airflow conditions and the airway wall temperature along the tract. To simulate normal breathing conditions, it is assumed that a CPAP device generates a positive pressure inside the patients' respiratory tract to keep the airways open during sleep. Hence, at rest, breathing is slower and more relaxed and the minute ventilation of a healthy adult, according to the literature, is experimentally determined at 9 L/min (Daigle et al., 2003). Previous research stated that the temperature and relative humidity of the microclimate between humans and bed covers (bed environment) are generally maintained around 29 °C and 65% respectively during normal sleep (Okamoto-Mizuno and Mizuno, 2012). To simulate CPAP conditions, the inlet flow rates to achieve the desired pressures inside the respiratory system are given by the device specifications (F&P, 2012). Hence, volume flow rates of 48.47, 53.95, 59.42 and 64.91 L/min are used to generate 5, 10, 15 and 20 cmH_2O of constant positive pressure. Then, knowing that the CPAP device operating principle is to introduce pressurized room air into the patient's respiratory system, the temperature and relative humidity inlet airflow conditions under CPAP conditions are set according to a room neutral sleeping environment, which corresponds to 22 °C and 50% respectively according to the literature (Lin and Deng, 2008). Hence, the inlet air water vapour concentration C_{A_0} is determined from the bed environment relative humidity for normal breathing conditions (65%) or room neutral sleeping environmental temperature for PAP conditions (50%) as $rHC_{A_{sat}}/100$. Where $C_{A_{sat}}$ is calculated from Eq. (3) using the inlet air temperature T_{A_0}, which is the bed environment temperature for normal breathing conditions (29 °C) or room neutral sleeping environmental temperature for PAP conditions (22 °C).

The wall temperature along the respiratory tract corresponds to the capillary blood temperature (T_B) on the basement membrane as a function of the distance from the nasal vestibule to the distal trachea. Because of the difficulty in obtaining accurate axial blood temperature distribution, T_B has been set as a linear distal increase at a 0.33 °C/cm rate from 32 °C at the nasal vestibule basement membrane temperature according to previous studies (Hanna and Scherer, 1986; Daviskas, Gonda and Anderson, 1990; Feng et al., 2016; Xi et al., 2016; Wu et al., 2014).

5. Parameters affected by CPAP application

There are two main effects that have to be extrapolated to the entire upper airways and considered to determine the geometrical airway diameter for each typical CPAP pressure of 5, 10, 15 and 20 cmH_2O CPAP simulation. These are the cell or epithelium compression and the ASL dryness or over-evaporation after CPAP application. Both effects are outlined in Fig. 3.

The positive pressure inside the upper airways generates a radial force normal to the epithelium in order to increase the volume of the airways, and as a consequence of this force, the epithelium is significantly compressed (from Fig. 3A–B). The epithelium compression is governed by the Bulk Modulus equation (6) which states that the pressure increase is proportional to the volume decrease, epithelial volume from normal breathing conditions ($\Delta P = 0$) to the desired CPAP ($\Delta P \neq 0$) in this case. The Bulk Modulus of respiratory epithelium is assumed constant for all pressures and modelled cylinders (Grau-Bartual et al., 2020). The equation can be written as a function of the epithelial circular crown area (*CCA*), since the axial segment length (L) is not affected by the radial positive force generated by the CPAP application, as follows:

$$B = -\frac{\Delta P}{\frac{\Delta V}{V_0}} = -\frac{\Delta P}{\frac{CCA'_{\Delta P}L - CCA_0 L}{CCA_0 L}} = -\frac{\Delta P}{\frac{y'_{Ep_{\Delta P}}(y'_{Ep_{\Delta P}} + D'_{\Delta P})}{y_{Ep_0}(y_{Ep_0} + D_0)} - 1} \quad (6)$$

The subsequent effect considered for extrapolation is the ASL dryness or over-evaporation (from Fig. 3B–C), which was quantified using two *in vitro* models in previous literature (Grau-Bartual et al., 2020). This is essential to determine the final airway dimensions at the desired CPAP ($\Delta P \neq 0$). It has been demonstrated that the air volume increase produced by CPAP hinders the natural air conditioning process and produces ASL dryness or over-evaporation. The water flux from the ASL layer to the airflow, which needs to achieve the proper relative humidity and reach the equilibrium, is higher when the pressure is applied. This is attributed to the fact that there is more air inside the respiratory system to be humidified than in normal breathing conditions. This increase in water flux produces a decrease in the ASL water content reservoir and hence in the ASL thickness.

Mathematically, according to the process outlined in Fig. 3B–C, the ASL thickness reduction ($\Delta y_{ASL\Delta P}$) can be expressed as $((y'_{ASL\Delta P} - y_{ASL\Delta P})/y'_{ASL\Delta P})$ and has been quantified for ΔP = 5, 10, 15 and 20 cmH_2O CPAP in previous literature (Grau-Bartual et al., 2020). Also, it is known that the ASL thickness (y_{ASL}) corresponds to 23% of the total epithelial thickness (y_{Ep}) according to the literature (Yu et al., 2006). Therefore, the epithelial thickness ($y_{Ep_{\Delta P}}$) at each specific CPAP pressure is written as follows:

$$y_{Ep_{\Delta P}} = 0.77y'_{Ep_{\Delta P}} + 0.23y'_{Ep_{\Delta P}} - (0.23y'_{Ep_{\Delta P}}\Delta y_{ASL_{\Delta P}}) \quad (7)$$

Finally, the airway diameter at each specific CPAP pressure ($D_{\Delta P}$) is written as $(D'_{\Delta P} + 2(y'_{Ep_{\Delta P}} - y_{Ep_{\Delta P}}))$. Where $D'_{\Delta P}$ corresponds to $(D_0 + 2(y_{Ep_0} - y'_{Ep_{\Delta P}}))$.

6. Computational strategy and statistics

The model is written, simulated and optimized on MATLAB R2014b (MathWorks®, NSW, Australia) and built-in functions, such as *ode*45 and *fsolve*, are used to solve the mathematical system. The governing equations are solved for each geometrical segment, and the output variables are used as input variables for the next segment. The same procedure is repeated for each CPAP setting as described in Fig. 4.

Statistical analysis was performed using GraphPad Prism software (GraphPad, San Diego, CA, USA) version 6.07 for windows using one-way analysis of variance (ANOVA), followed by Tukey

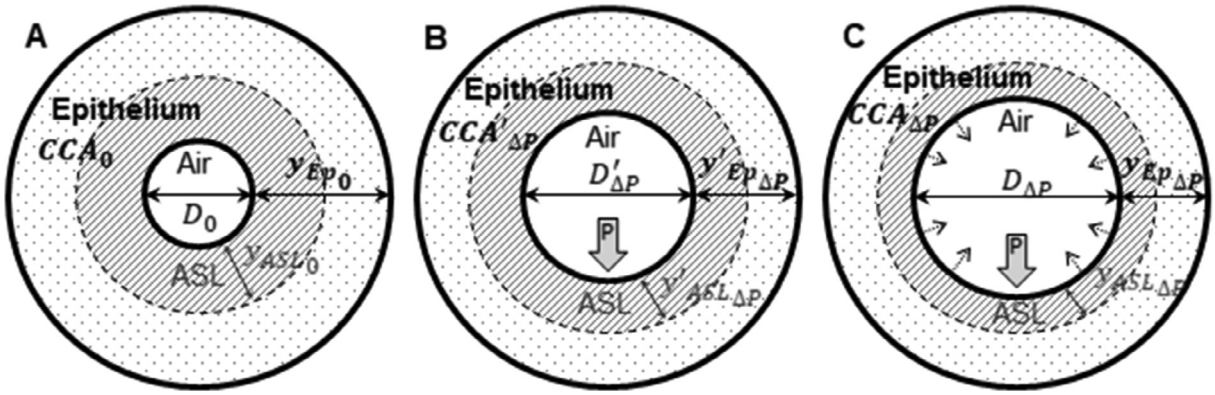

Fig. 3. Schematic representation of the dimensions' evolution cylinder-based airway radial plane when CPAP is applied. (A) Initial airway dimensions which corresponds to normal breathing conditions ($\Delta P = 0$). (B) Airway dimensions evolution when CPAP is applied due to tissue compression. Epithelium and ASL layers are assumed equally compressed. (C) Representation of the drying effect when CPAP is applied, where the ASL layer thickness is also reduced due to the water transfer from the ASL layer to the airflow in order to achieve the air conditioning process.

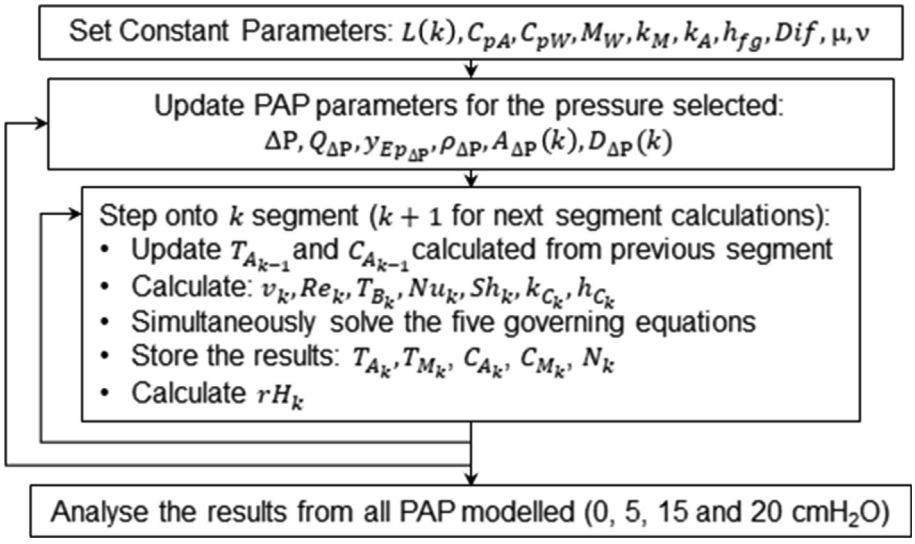

Fig. 4. Flow diagram of upper airway PAP model outlining the steps to follow to compare the governing state parameters evolution at each PAP selected valid from 0 to 20 cmH2O.

post hoc analysis for multiple comparisons (* $p < 0.05$, ** $p < 0.01$, *** $p < 0.001$ and **** $p < 0.0001$).

7. Heat and water transport CPAP model results

The evolution of the five state variables (T_A, T_M, C_A, C_M, N) and the airflow relative humidity (rH) along the upper airways have been analysed and compared for each pressure scenario simulated. The relative humidity has been included in the results because it is an indicative parameter of the external humidification needed in the CPAP compressed air to overcome the dryness side effect reported by patients.

The mean temperature, water vapour concentration, water flux from the ASL layer to the airflow and relative humidity evolution in the airflow as a function of the upper airways distance or airway cylinder number (T_M, C_M, N and rH respectively) are represented in Fig. 5A, B, C and D respectively.

The results show a significant reduction in airflow temperature (average of 5 °C) and water vapour concentration (average of 5 mg/L) for each pressure applied compared to normal breathing conditions (control at $\Delta P = 0$). The water flux is the transport of water molecules from the ASL to the airflow as a function of area and time, and it is the parameter used to quantify the mass transfer effect, water transfer in our study. It is significantly greater when the pressure is applied, which means that the liquid water reservoir on the ASL layer has to be greater than in normal conditions ($\Delta P = 0$) in order to have enough water to achieve the thermodynamic liquid–vapour phase equilibrium on the ASL outer surface and prevent ASL dryness. The amount of water supplied to the airflow to achieve air conditioning and hence equilibrium is determined by the water flux (N) from the ASL layer to the airflow. The water flux (N) values do not follow an upward trend as the other parameters. In this graph significant peaks can be observed on the nasal turbinate, distal nasopharynx and larynx. These are the narrowest sections in the upper airway geometry. Hence, these areas are with the highest turbulent flow and water transfer rate from the mucus to the airflow. The mean airway relative humidity is a parameter calculated from the mean airway water concentration and temperature, and represents the amount of water vapour present in the airflow at each upper airway section (cylinder). It is also significantly reduced after CPAP application and noticeable at higher pressures.

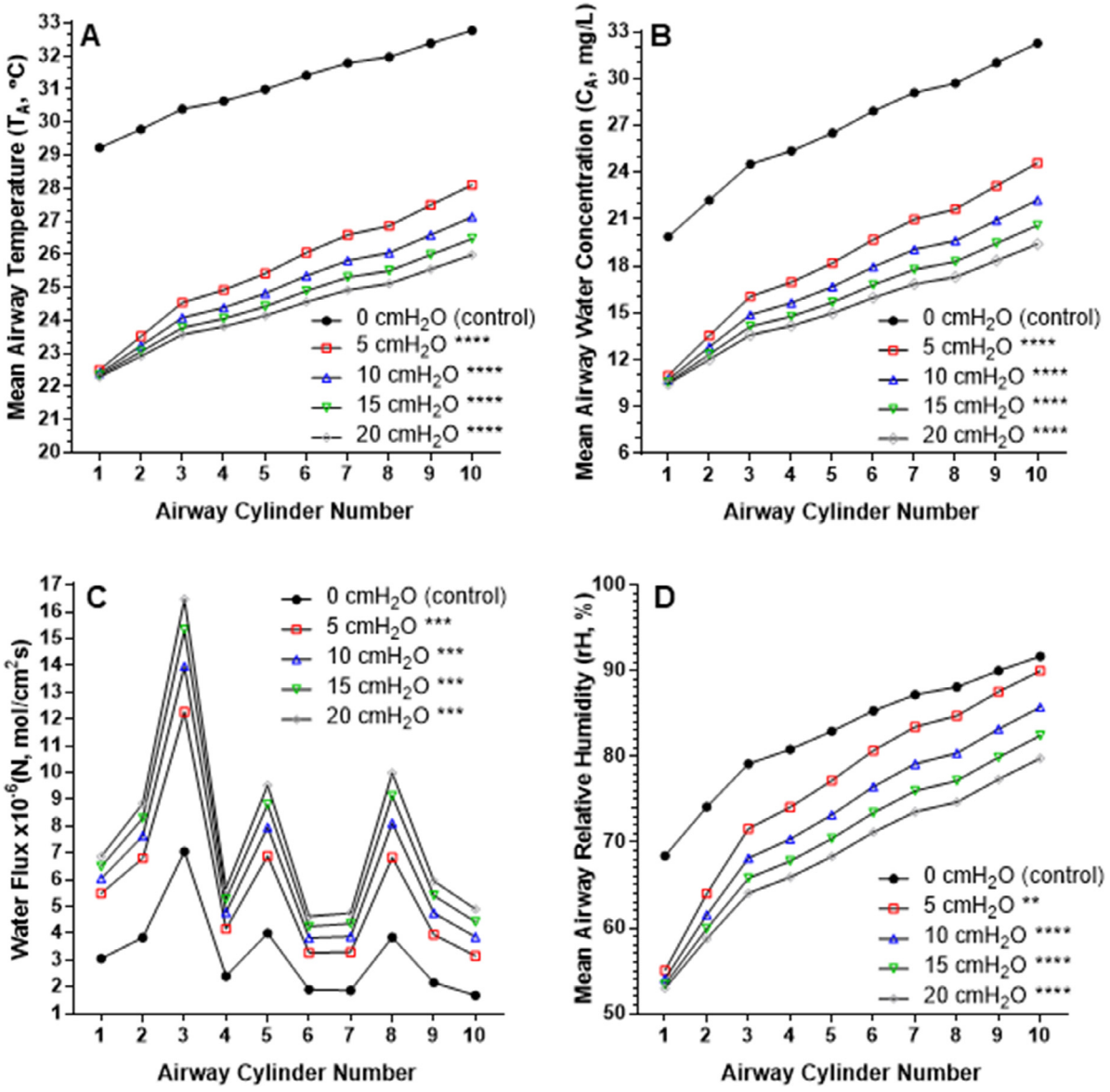

Fig. 5. Evolution of mean airflow temperature (A), water vapour concentration (B), water flux (C) and relative humidity (D) along the upper airway cylinder at ΔP = 0, 5, 10, 15 and 20 cmH2O. 1 – Nasal Vestibule, 2 – Nasal Cavity, 3 – Nasal Turbinate, 4 – Proximal Nasopharynx, 5 – Distal Nasopharynx, 6 – Oropharynx, 7 – Hypopharynx, 8 – Larynx, 9 – Proximal trachea, 10 – Distal trachea. One-way ANOVA statistical analysis followed by Tukey post hoc analysis for multiple comparisons (**p < 0.01, ***p < 0.001 and ****p < 0.0001).

8. Heat and water transport CPAP model validation

The temperature and water concentration in mean airflow, water flux and relative humidity evolution as a function of the upper airway distance obtained from the mathematical model under normal breathing conditions (control at ΔP = 0) are in agreement with the inspiration airflow evolution obtained in air-conditioning models previously developed on the literature (Reinikainen and Jaakkola, 2003; F&P, 2012; Hanna and Scherer, 1986; Daviskas, Gonda and Anderson, 1990; Feng et al., 2016; Xi et al., 2016; Wu et al., 2014; McFadden et al., 1985).

The results obtained for each pressure condition (5, 10, 15 and 20 cmH_2O) have been compared with the experimental results obtained in two human epithelial cell lines, Calu-3 and RPMI 2650 cells, *in vitro* models. Based on the law of conservation of mass, it is possible to state that the ASL layer thickness reduction quantified experimentally (Grau-Bartual et al., 2020) corresponds to the amount of water molecules transferred from the ASL layer to the airflow, which is the water flux. Hence, model validation is achieved comparing the flux increase of water molecules transferred from the ASL layer to the airflow (N) due to ΔP increase determined theoretically with the mathematical human upper airway CPAP model, with the ASL thickness ($\Delta y_{ASL\Delta P}$) reduction quantified experimentally after each CPAP application (Grau-Bartual et al., 2020).

To determine the flux increase as a function of the pressure variation, the water flux average is calculated from all model sections (cylinders) at each pressure (N_{AV}). Then, the dimensionless increase is calculated from the water flux average at ΔP = 0 cmH_2O (control) (N_{AV_0}) to the water flux average at ΔP ≠ 0 (PAP application) ($N_{AV_{\Delta P}}$), as described in the first part of equation (8).

$$N_{Increase} \approx \left(\frac{N_{AV_{\Delta P}} - N_{AV_0}}{N_{AV_0}}\right)_{Theoretical} \approx \left(\frac{\Delta TEER_{\Delta P} - \Delta TEER_0}{\Delta TEER_0}\right)_{Experimental} \quad (8)$$

The experimental water flux increases due to ASL thickness decrease as a function of the pressure variation (Grau-Bartual et al., 2020). Briefly, ASL thickness reduction, water content reduction or dryness of the *in vitro* epithelium after CPAP application were determined using an electric cell-substrate impedance sensing apparatus with a medium frequency of 4000 Hz which allows the current pathway to pass through both the cell membrane and junctions and provide the trans-epithelial electrical resistance (TEER). By definition, the pure electrical resistance is proportional to the distance between the electrodes or the thickness of the conductor material. Hence, the TEER values are proportional to the cell layer thickness, since the cell temperature, the effective area of the *in vitro* epithelium and the cell layer electrical resistivity are constant in all of the experiments. The measured TEER values are compared between the 70%rH and 100%rH scenarios at specific pressure with the control measurement (no CPAP application, $\Delta P = 0$) as described in the second part of equation (8).

The resulting theoretical and experimental water flux increase as a function of the pressure variation (ΔP) on both epithelial cell *in vitro* models, Calu-3 and RPMI 2650 cells, are shown in Fig. 6.

The results show a similar water flux rise trend proportional to the increase in pressure application. No significant difference is found between the theoretical or experimental results at each pressure ($p > 0.05$), which corroborates the similarity of the results and validates the model.

9. Heat and water transport CPAP model input optimization

The mathematical model described is used to determine the optimal input temperature and relative humidity in the CPAP humidifier to overcome the dryness side effect and improve the comfort and the acceptance of CPAP patients.

The main airway temperature, water concentration, relative humidity and water flux evolution along the upper airway simulated for normal breathing conditions (Control, $\Delta P = 0$), using the inlet parameters set at 29 °C and 65%rH for bed environment conditions, have been considered as a reference. Then the inlet parameters for each pressure scenario have been increased, starting from the neutral sleeping environmental conditions 22 °C and 50%rH, until no significant difference is found between the new main airway temperature, water concentration, relative humidity and water flux evolution along the upper airway and the reference results (Control, $\Delta P = 0$).

The optimum inlet conditions for each pressure analysed are presented in Table 1, and the resulting main airway temperature, water concentration, relative humidity and water flux evolution along the upper airway obtained using the optimum inlet air temperature and water concentration for each pressure are shown in Fig. 7. The statistical analysis to determine the optimal values is performed considering the data for each pressure as an individual group. The aim of the simulation is to reach no significances ($p > 0.05$) between the airflow temperature and water concentration in the airflow and their corresponding controls in any of the pressures simulated after the proximal trachea. The objective is successfully achieved showing no significant differences in any of the resulting parameters after the 9th cylinder.

10. Model limitations

To facilitate model development, assumptions and simplifications have been made to reduce computational complexity whilst maintaining the governing process characteristics. The geometry of the human upper airways has been approximated to an idealized symmetric cylinder-based airway model devoid of realistic anatomical detail of the nasopharynx. The airflow process is considered 1D, time-independent, steady, and fully developed, simulating only inspiratory phase, hence the gas is moving from the nares to the trachea. The model is formulated to simulate only a nasal respiration and is solved for steady-state conditions.

11. Discussion

The purpose of this study was to develop a simple, efficient, fast computing and realistic 1D upper airway representation able to predict the heat and water transfer variation between normal breathing and CPAP conditions based on mass and heat transfer equations. The initial heat and water transport CPAP model results show a significant reduction in the airflow temperature and water

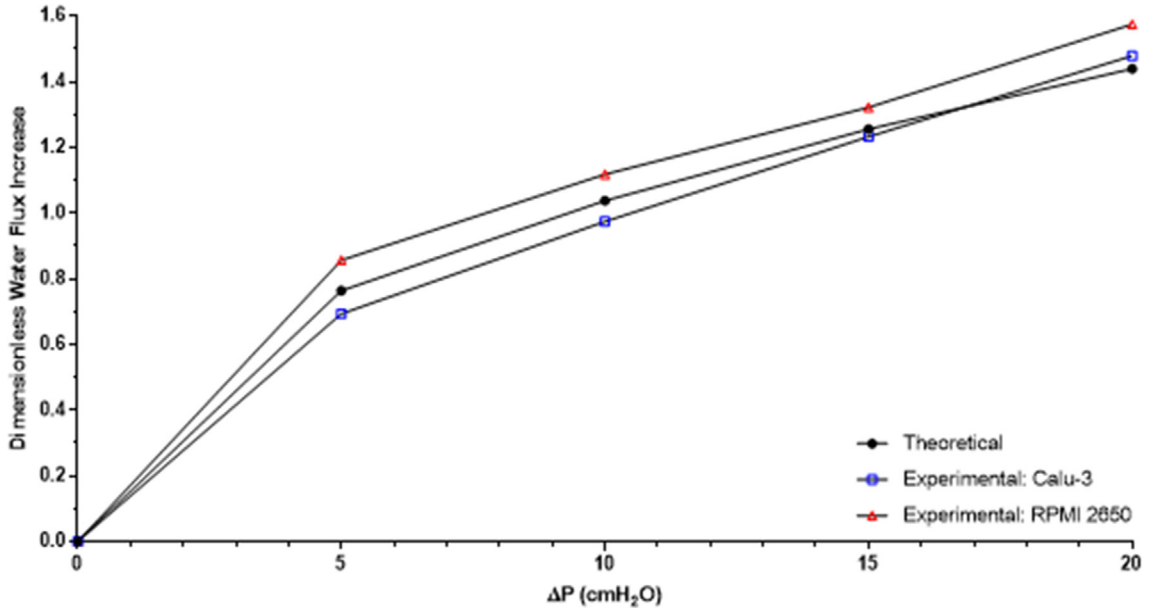

Fig. 6. Theoretical and experimental, from Calu-3 and RPMI 2650 cells lines, dimensionless water flux increase as a function of pressure variation (ΔP). One-way ANOVA statistical analysis ($p > 0.05$). No significant difference is found on the results which validates the theoretical model.

Table 1
Optimal inlet airflow temperature (T_{A_0}), relative humidity (rH_0) and water vapour concentration (C_{A_0}) for each PAP application analysed.

ΔP (cmH_2O)	T_{A_0} (°C)	rH_0 (%)	C_{A_0} (mg/L)
5	30.5	77.5	24.15
10	31	81.5	26.08
15	31.5	84	27.62
20	32	85.5	28.87

vapour concentration for each CPAP simulated compared to normal breathing conditions (control at $\Delta P = 0$), which are more disparate at higher pressures. Regarding water transfer from the ASL layer to the compressed airflow, the water flux as a function of area and time is significantly greater when the pressure is applied. The mean airway relative humidity is also significantly reduced after CPAP application and noticeable at higher pressures. These results agree with the dryness side-effects reported by OSA patients after CPAP therapy, and are attributed to the fact that the therapy deforms the respiratory epithelium and inhibit the upper airways natural air conditioning process. CPAP generates airflow and positive pressure to keep the airways open. While the former could provoke over-evaporation of ASL water content, the latter may compress the epithelium and block the goblet cells or mucus secretion glands, as reported in previous studies (Grau-Bartual et al., 2020).

The resulting mathematical model has been validated with previous *in vitro* results (Grau-Bartual et al., 2020) and the model input variables (inlet airflow temperature and water concentration) have been optimized to approximate the previous state variables obtained under the different pressures analysed ($\Delta P \neq 0$) to the normal breathing conditions where no pressure is applied ($\Delta P = 0$). The obtained data can be used as an indication to confirm that humidification with CPAP is absolutely necessary to alleviate

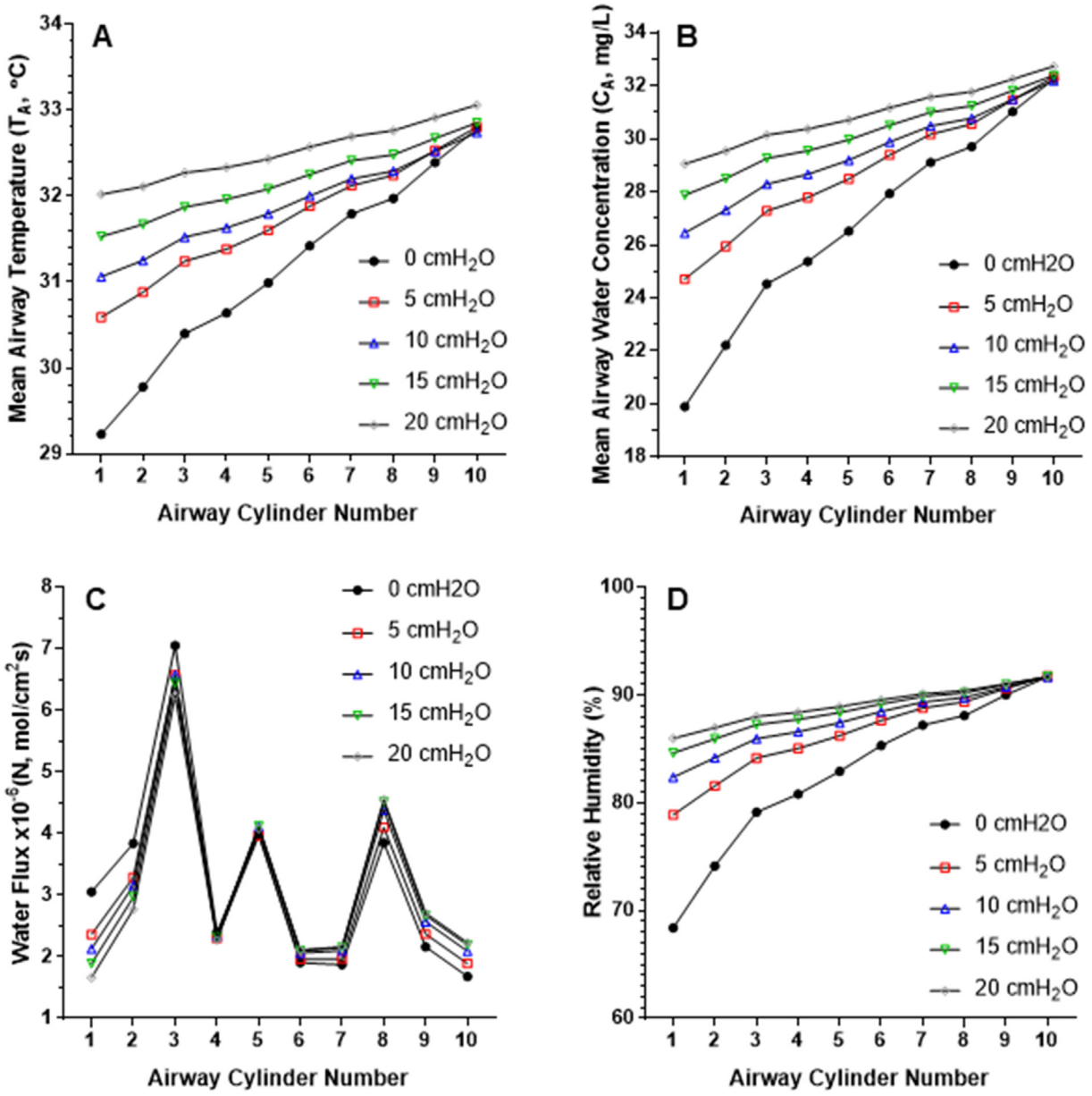

Fig. 7. Evolution of mean airflow temperature (A), water vapour concentration (B), water flux (C) and relative humidity (D) along the upper airway cylinder at $\Delta P = 0, 5, 10, 15$ and 20 cmH_2O using optimum inlet conditions. (1) – Nasal Vestibule, 2 – Nasal Cavity, 3 – Nasal Turbinate, 4 – Proximal Nasopharynx, 5 – Distal Nasopharynx, 6 – Oropharynx, 7 – Hypopharynx, 8 – Larynx, 9 – Proximal trachea, 10 – Distal trachea. No significant difference is found on the results after the proximal trachea. One-way ANOVA statistical analysis followed by Tukey post hoc analysis for multiple comparisons ($p > 0.05$).

upper airways dryness, and initially set the humidifier conditions according to the CPAP titration pressure. Additionally, the mathematical model described in this study can be used to customize the temperature and humidity targeted for each patient, and simulate the effect of other breathing disorders such as asthma, or viruses affecting the respiratory tract such as COVID-19.

Declaration of Competing Interest

The authors declare that they have no known competing financial interests or personal relationships that could have appeared to influence the work reported in this paper.

Acknowledgements

The authors acknowledge the Auckland University of Technology for the Vice Chancellor's Doctoral Scholarship and AUT Institute of Biomedical Technologies for the financial support. Dr Sandra Grau-Bartual has contributed to the development of the model, validation, drafting the paper, analysis and discussion. Professor Al-Jumaily has contributed to the concept, development of the model, discussion and approving it.

Appendix A. Summary of parameters

Although all the parameters and variables are included in the list of abbreviations and symbols, the parameters used to formulate the human upper airway CPAP model are also summarized in the following tables for simplicity. They are divided in three main groups: geometrical parameters, constant variables and variables.

Geometrical parameters

See Table A1.

Table A1
Geometrical parameters used to formulate the human upper airway CPAP model. It contains the symbol of each parameter, a brief description, mathematical value and unit and the reference number.

Parameters	Description	Value	Units
$\boldsymbol{L(k)}$	UA Length Vector	[2.0 4.0 4.0 1.4 1.9 2.3 2.1 1.1 2.7 2.8]	cm
$\boldsymbol{D_0(k)}$	UA Diameter Vector at $\Delta P = 0$	[1.5 1.2 0.6 2.0 1.2 2.5 2.4 1.1 1.8 2.1]	cm
$\boldsymbol{y_0}$	Epithelium Thickness at $\Delta P = 0$	65	nm

Constant variables

See Table A2.

Table A2
Constant parameters used to formulate the human upper airway PAP model. It contains the symbol of each parameter, a brief description, mathematical value and unit and the reference number.

Variables	Description	Value	Units
$\boldsymbol{\Delta P}$	Positive airway Pressure Increase	0, 5, 10, 15, 20	cmH_2O
$\boldsymbol{Q_0}$	Airflow Rate at $\Delta P = 0$ cmH_2O	150	cm^3/s
$\boldsymbol{Q_5}$	Airflow Rate at $\Delta P = 5$ cmH_2O	241.25	cm^3/s
$\boldsymbol{Q_{10}}$	Airflow Rate at $\Delta P = 10$ cmH_2O	332.5	cm^3/s
$\boldsymbol{Q_{15}}$	Airflow Rate at $\Delta P = 15$ cmH_2O	423.75	cm^3/s
$\boldsymbol{Q_{20}}$	Airflow Rate at $\Delta P = 20$ cmH_2O	515	cm^3/s

Table A2 (*continued*)

Variables	Description	Value	Units
$\boldsymbol{k_M}$	Epithelial and ASL Thermal Conductivity	0.00144	cal/cm s K
$\boldsymbol{k_A}$	Moist Air Thermal Conductivity	6.432e-5	cal/cm s K
$\boldsymbol{h_{fg}}$	Latent heat of vaporization	578.4	cal/g
$\boldsymbol{M_W}$	Water Molecular Weight	18.016	g/mol
$\boldsymbol{Dif}$	Diffusivity of Water Vapour in Air	0.27	cm^2/s
$\boldsymbol{\rho}$	Density of Moist Air	0.00112	g/cm^3
$\boldsymbol{\mu}$	Dynamic Viscosity of Moist Air	1.846e-4	cal/cm s K
$\boldsymbol{C_{pA}}$	Moist Air Heat Capacity at Constant Pressure	0.2592	cal/g K
$\boldsymbol{C_{pW}}$	Water Heat Capacity at Constant Pressure	1	cal/g K
$\boldsymbol{R}$	Ideal Gas Constant	8.31	m^3Pa/mol K
$\boldsymbol{B}$	Bulk Modulus of Respiratory Epithelium	10,500	Pa

Variables

See Table A3.

Table A3
Variables used to formulate the human upper airway CPAP model. It contains the symbol of each parameter, a brief description and the unit of measure.

Variables	Description	Units
$\boldsymbol{T_{A_k}}$	Local Airflow Temperature	K
$\boldsymbol{T_{M_k}}$	Local Mucus Temperature at the ASL Outer Surface	K
$\boldsymbol{T_{B_k}}$	Local Blood Temperature at the Basement Capillary Membrane	K
$\boldsymbol{C_{A_k}}$	Local Airflow Water Vapour Concentration	mol/cm^3
$\boldsymbol{C_{M_k}}$	Local Saturation Water Vapour Concentration at the ASL Outer Surface	mol/cm^3
$\boldsymbol{N_k}$	Local Water Transfer Rate from the ASL Outer Surface to the Airflow	mol/cm^3 s
$\boldsymbol{v_k}$	Local Airflow Velocity	cm/s
$\boldsymbol{A_k}$	Local Cross-Sectional Area	cm^2
$\boldsymbol{Nu_k}$	Local Dimensionless Nusselt Number	–
$\boldsymbol{Re_k}$	Local Dimensionless Reynolds Number	–
$\boldsymbol{Sh_k}$	Local Dimensionless Sherwood Number	–
$\boldsymbol{k_{C_k}}$	Local Mass Transfer Coefficient	cm/s
$\boldsymbol{h_{C_k}}$	Local Heat Transfer Coefficient	cal/cm^2 s K
$\boldsymbol{P_{sat_k}}$	Tetens Saturation Pressure	Pa
$\boldsymbol{rH_k}$	Relative Humidity	%

References

Al-Jumaily, A.M., Mithraratne, P., Gradon, L., White, D., 2003. Modelling and simulation of a breathing system. In: ASME 2003 International Mechanical Engineering Congress and Exposition, IMECE2003-41853, pp. 1209–1214.
Buck, A.L., 1981. New equations for computing vapor pressure and enhancement factor. J. Appl. Meteor. 20 (12), 1527–1532.
Daigle, C.C., Chalupa, D.C., Gibb, F.R., Morrow, P.E., Oberdörster, G., Utell, M.J., Frampton, M.W., 2003. Ultrafine particle deposition in humans during rest and exercise. Inhalat. Toxicol. 15 (6), 539–552.
Daviskas, E., Gonda, I., Anderson, S.D., 1990. Mathematical modeling of heat and water transport in human respiratory tract. J. Appl. Physiol. 69 (1), 362–372.
Even-Tzur, N., Kloog, Y., Wolf, M., Elad, D., 2008. Mucus secretion and cytoskeletal modifications in cultured nasal epithelial cells exposed to wall shear stresses. Biophys. J. 95 (6), 2998–3008.
Feng, Y.u., Kleinstreuer, C., Castro, N., Rostami, A., 2016. Computational transport, phase change and deposition analysis of inhaled multicomponent droplet–vapor mixtures in an idealized human upper lung model. J. Aerosol Sci. 96, 96–123.
Fisher, and, Paykel, and Healthcare, 2012. Icon TM + Novo: Use and Care Manual. Auckland, NZ.
Grau-Bartual, S., Al-Jumaily, A.M., Young, P.M., Traini, D., Ghadiri, M., 2020. Effect of continuous positive airway pressure treatment on permeability, inflammation and mucus production of human epithelial cells. ERJ Open Res. 2020 (6), 00327–2019.
Guimaraes, K.C., Drager, L.F., Genta, P.R., Marcondes, B.F., Lorenzi-Filho, G., 2009. Effects of oropharyngeal exercises on patients with moderate obstructive sleep apnea syndrome. Am. J. Respir. Crit. Care Med. 179 (10), 962–966.

Hanna, L.M., Scherer, P.W., 1986. A theoretical model of localized heat and water vapor transport in the human respiratory tract. J. Biomech. Eng. 108 (1), 19–27.
Kreda, S.M., Okada, S.F., van Heusden, C.A., O'Neal, W., Gabriel, S., Abdullah, L., Davis, C.W., Boucher, R.C., Lazarowski, E.R., 2007. Coordinated release of nucleotides and mucin from human airway epithelial Calu-3 cells. J. Physiol. 584 (Pt 1), 245–259.
Lin, Z., Deng, S., 2008. A study on the thermal comfort in sleeping environments in the subtropics—Developing a thermal comfort model for sleeping environments. Build. Environ. 43 (1), 70–81.
Malik, N.W., Kenyon, G.S., 2004. Changes in the nasal airway mucosa and in nasal symptoms following continuous positive airway pressure (N-CPAP) for obstructive sleep apnea. Aust. J. Otolaryng. 7 (1), 17–20.
McFadden Jr., E.R., Pichurko, B.M., Bowman, H.F., Ingenito, E., Burns, S., Dowling, N., Solway, J., 1985. Thermal mapping of the airways in humans. J. Appl. Physiol. 58 (2), 564–570.
Okamoto-Mizuno, Kazue, Mizuno, Koh, 2012. Effects of thermal environment on sleep and circadian rhythm. J. Physiol. Anthropol. 31 (1).
Reinikainen, L.M., Jaakkola, J.J.K., 2003. Significance of humidity and temperature on skin and upper airway symptoms. Indoor Air 13, 334–352.
The anatomy and body, 2018. The upper respiratory tract.
West, J.B., 2013. Pulmonary Pathophysiology: The Essentials (Eighth). Lippincott Williams & Wilkins, USA.
Wolf, M., Naftali, S., Schroter, R.C., Elad, D., 2004. Air-conditioning characteristics of the human nose. J. Laryngol. Otol. 118, 87–92.
Wu, D., Tawhai, M.H., Hoffman, E.A., Lin, C.-L., 2014. A numerical study of heat and water vapor transfer in MDCT-based human airway models. Ann. Biomed. Eng. 42 (10), 2117–2131.
Xi, J., Kim, J., Si, X.A., 2016. Effects of nostril orientation on airflow dynamics, heat exchange, and particle depositions in human noses. Eur. J. Mech. B. Fluids 55, 215–228.
Yeager, H., 1971. Tracheobronchial secretions. Chest 50, 493–509.
Yu, K.N., Lau, B.M.F., Nikezic, D., 2006. Assessment of environmental radon hazard using human respiratory tract models. J. Hazard. Mater. 132 (1), 98–110.